Supporting Information

Influence of the tumor microenvironment on ^{18}F-FDG uptake: A single-cell imaging study

Silvan Türkcan*, Louise Kiru*, Dominik Naczynski, Laura Sasportas, and Guillem Pratx
* *Equal contribution*

Image Analysis and Quantitation: Radioluminescence images were obtained by our methodology called "optical reconstruction of the beta-ionization track" (ORBIT) as described in detail in Pratx *et al.* [1] (Fig. S1 B). Briefly, after image acquisition, each frame is first filtered with a Gaussian kernel to reduce spatially uncorrelated shot noise. The processed image is later segmented using a constant threshold set above the noise floor. The final ORBIT image is reconstructed by aggregating the center of mass of each detected track for every image. The resulting image is then filtered with a Gaussian kernel to account for the localization uncertainty.

In results reported here, the number of FDG molecules refers to the number of molecules present at the beginning of the acquisition, inferred from the number of observed decays. It can be obtained from the standard decay equation for radioisotopes $A(t) = A_0 \exp(-\lambda t)$, where A is the time-varying activity and λ is the rate constant of radioactive decay, which is related to the half-life, $t_{1/2}$, by the expression $\lambda = \ln(2) / t_{1/2}$. When both sides are integrated over the total observation time T, the left side of the equation yields the number of observed decays N during this time. Solving the expression for the initial radioactivity $A(0)$ and converting it to the initial number of molecules N_0 via $N_0=A_0/\lambda$ gives an expression for the initial number of observed FDG molecules, which we use throughout this work:

$$N_0 = \frac{N}{1 - e^{-\lambda T}} \frac{1}{\text{yield}} \frac{1}{\text{eff}}$$

The yield factor accounts for the fact that the decay of ^{18}F yields a positron only 97% of the time. The remaining decays occur by electron capture, which is not observable by radioluminescence microscopy. The efficiency factor (eff) is 0.37 and includes the capture efficiency of the LV200 microscope set-up and the reconstruction algorithm. It was determined by imaging a known ^{18}F concentration on the microscope.

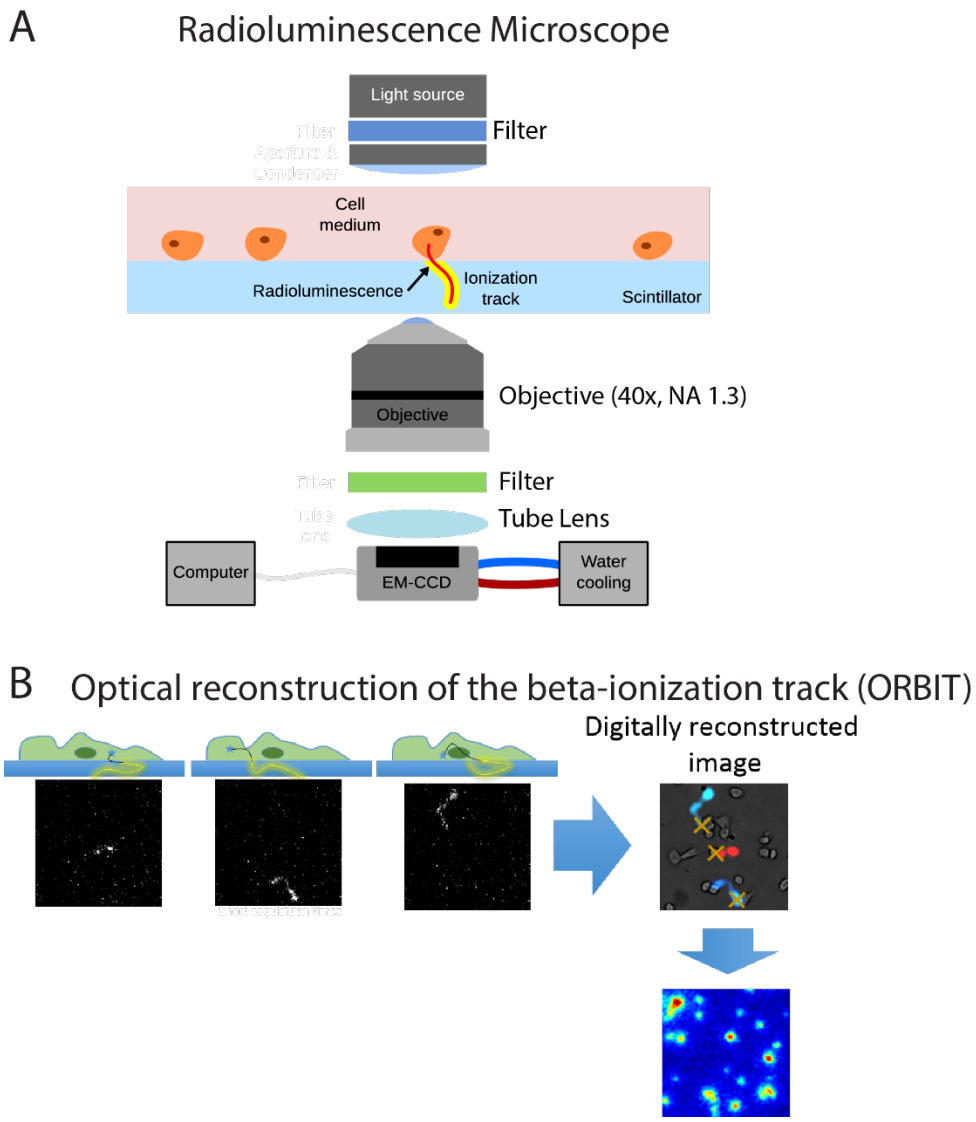

Figure S1. Schematics of the radioluminescence microscope and image reconstruction. (**A**) Upon decay of a ^{18}F nucleus, a β-particle is emitted and travels into the scintillator, up to several hundred microns. In response to the energy deposited by the particle, the scintillator emits visible photons along the trajectory of the β-particle, which are collected by a high NA microscope (Olympus LV200). (**B**) The radioluminescence image was obtained by our methodology called "optical reconstruction of the beta-ionization track" (ORBIT) as described in detail in Pratx *et al.* [1] and in the methods section. Individual decays are imaged with a high acquisition time and their center of mass is recorded to build up a 2D histogram of decays, which digitally represent the distribution of the ^{18}F-FDG molecules within the field of view.

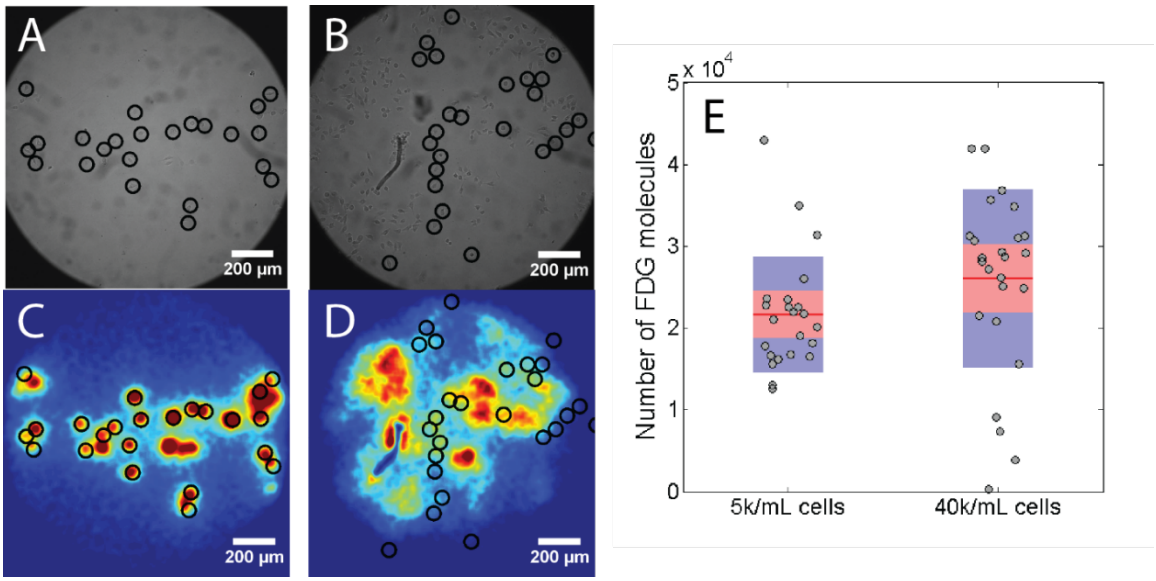

Figure S2. Influence of cell density on FDG uptake. (**A**, **B**) Bright field images of the MDA-MB-231 cells seeded at a density of 5,000 and 40,000 cells per mL, respectively, and (**C**, **D**) corresponding FDG images and selected cells. (**E**) Number of FDG molecules in selected single cells for the two seeding concentrations. The two populations do not differ significantly in FDG uptake.

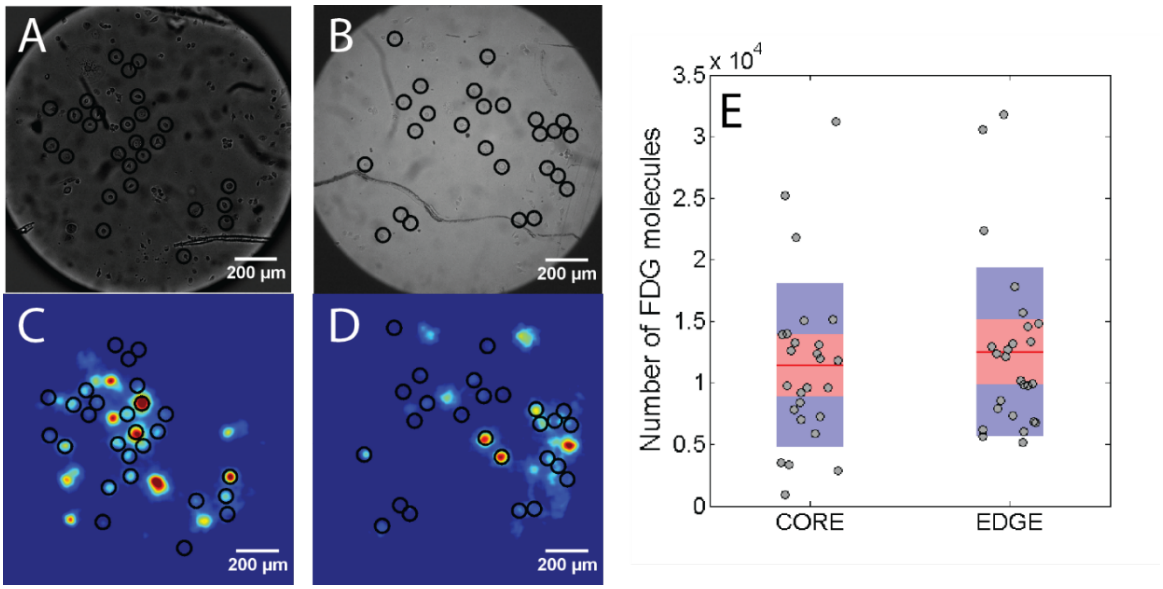

Figure S3. Loss of core/periphery phenotype after three weeks in culture. Cells from the core and periphery were passaged in culture for 3 weeks prior to imaging. (**A**, **B**) Brightfield images of MDA-MB-231 cells from tumor core and periphery (edge) and (**C**, **D**) corresponding FDG images and selected cells. (**E**) Number of FDG molecules in the selected individual MDA-MB-231 cells for cells from the core and the periphery. The two populations have similar FDG uptake after they have been in culture for three weeks.

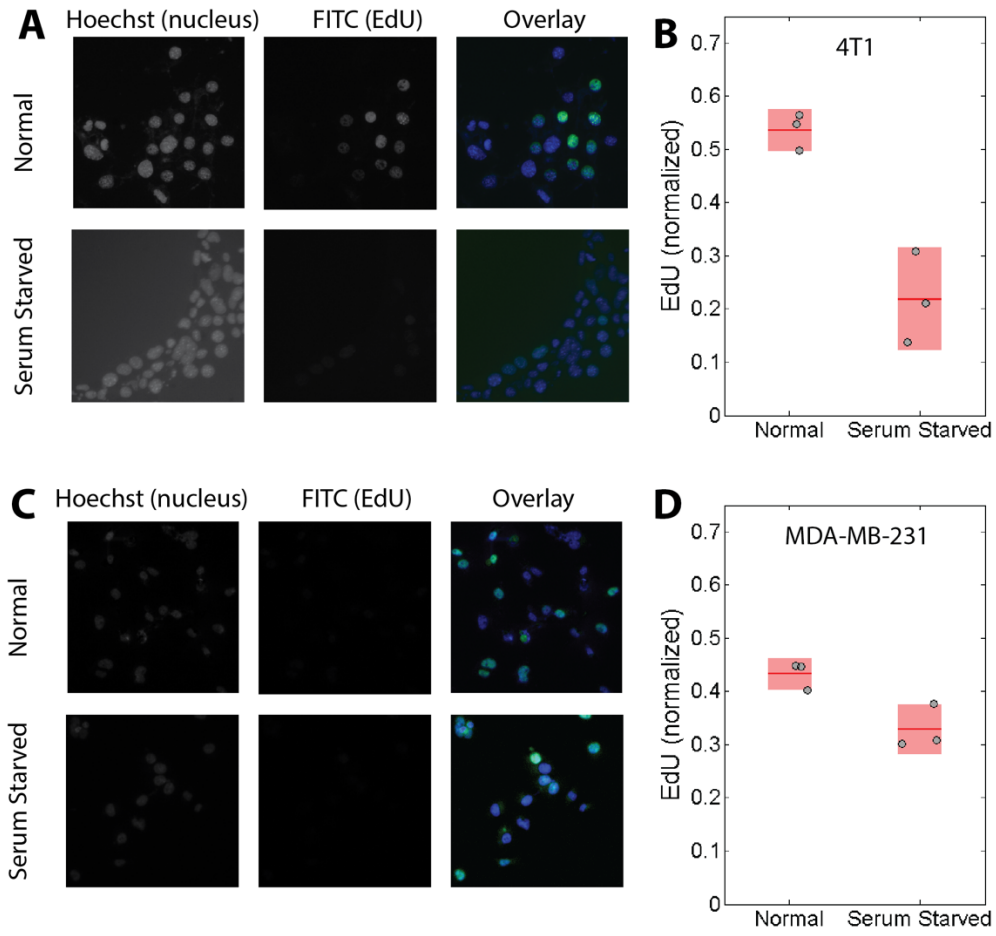

Figure S4. Cell proliferation after serum withdrawal (48h) measured using EdU incorporation into DNA. (**A**, **B**) Fluorescence microscopy and quantitation of the fraction of cells displaying positive EdU incorporation for 4T1 cells. (**C**, **D**) Same, for MDA-MB-231 cells. Significant cell arrest can be seen after serum is removed.

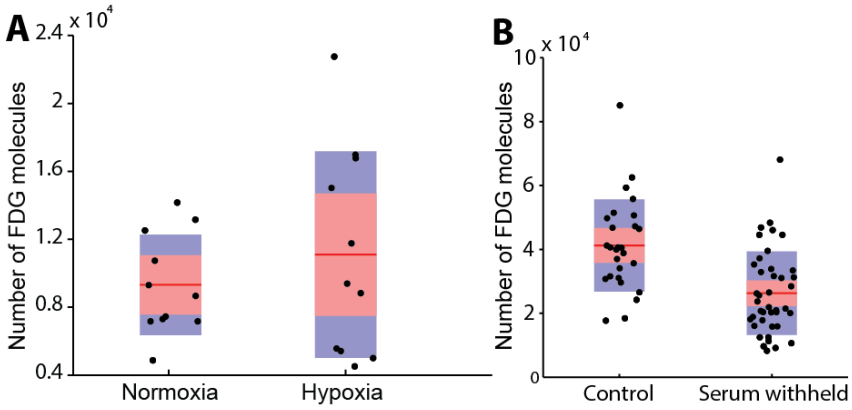

Figure S5. *In vitro* FDG uptake for different environmental conditions, for MDA-MB-231 cells. (**A**) Single-cell FDG uptake under normoxia and chronic hypoxia (2 % O_2, 7 days). FDG uptake increased 20% but the increase was not significant. (**B**) Single-cell FDG uptake with and without serum (48h). Serum-starved MDA-MB-231 cells took up 37% less FDG (P=0.002).

Table S1. FDG Uptake in Cells from Core and Periphery of Tumor Graft

Cell Line	Tumor size (mm)	FDG mol. ×1000 / cell (core)	N	FDG mol. ×1000 / cell (peri.)	N	Diff. (%)	P	CV^{+}_{Core}	CVP_{eri}
4T1	8.3	8.4 ± 2.0 (0.5)∗	18	12.0 ± 4.0 (0.8)	29	38	0.007	0.23	0.37
4T1	7.0	5.5 ± 3.0 (0.7)	25	4.9 ± 2.0 (0.3)	28	-11	NS	0.59	0.36
4T1	11.7	3.1 ± 1.3 (0.2)	43	4.4 ± 1.5 (0.3)	28	29	0.0004	0.42	0.35
4T1	12.5	1.5 ± 0.8 (0.2)	29	2.7 ± 1.5 (0.4)	17	43	0.045	0.54	0.56
4T1	14.5	3.7 ± 2.0 (0.4)	29	11.0 ± 5.0 (1.2)	17	68	$<10^{-5}$	0.62	0.43
4T1	15.5	18.6 ± 10.0 (1.7)	33	25.0 ± 10.0 (2.0)	35	26	0.017	0.52	0.46
MDA-MB-231	17	3.3 ± 4.0 (1.2)	10	22.5 ± 10.0 (1.7)	35	84	10^{-6}	1.18	0.45
MDA-MB-231	5.7	6.5 ± 2.0 (0.5)	25	7.4 ± 3.0 (0.7)	17	13	NS	0.37	0.43
MDA-MB-231	13.3	5.8 ± 4.0 (0.9)	17	14.0 ± 9.0 (2.0)	29	60	$<10^{-3}$	0.65	0.60

∗ Mean ± standard deviation (standard error of the mean)

+ Coefficient of variation (CV) measures intrapopulation heterogeneity of FDG uptake

Table S2. qPCR gene expression of a panel of hypoxia-related genes normalized using all housekeeping genes (ABI OneStepPlus, Quiagen RT2). The genes shown are those with 3-fold expression in the core of the tumor compared to the periphery.

GENE	FOLD CHANGE	GENE	FOLD CHANGE
Epo	41.8	Nos3	5.5
Hnf4a	27.4	Edn1	5.2
Hif3a	13.2	F3	3.8
Adm	12.0	Adora2b	3.5
Pfkfb3	9.9	Bhlhe40	3.3
Angptl4	8.9	Hif1an	3.1
F10	7.1	Serpine1	3.0
Slc2a3	6.2		

Table S3. FDG Uptake in Single Cells under Chronic Hypoxia

Cell Line	FDG mol. ×1000 / cell (normoxic)	N	FDG mol. ×1000 / cell (hypoxic)	N	Diff. (%)	*P*	$CV^{+}_{normoxic}$	$CV_{hypoxic}$
4T1	9.8 ± 3.6 (1.0)*	14	26.5 ± 9.0 (2.7)	11	171	$<10^{-4}$	0.37	0.34
MDA-MB-231	9.3 ± 3.0 (0.9)	11	11.1 ± 6.1 (1.8)	11	20	NS	0.32	0.55

∗ Mean ± SD (SEM)

+ Coefficient of variation

Table S4. FDG Uptake in Single Cells Grown Serum-Free

Cell Line	FDG mol. ×1000 / cell (10% serum)	N	FDG mol. ×1000 / cell (0% serum)	N	Diff. (%)	*P*	$CV^{+}_{control}$	$CV_{starved}$
4T1	19 ± 10 (2)∗	29	7 ± 3 (1.1)	8	63	0.004	0.53	0.46
MDA-MB-231	55 ± 20 (4)	27	35 ± 16 (3)	41	37	0.002	0.34	0.48

∗ Mean ± SD (SEM)

+ Coefficient of variation

Table S5. FDG Uptake in Single Cells Grown Under High Lactate

Cell Line	FDG mol. ×1000 / cell (No lactate)	N	FDG mol. ×1000 / cell (30 mM lactate)	N	Diff. (%)	*P*	$CV^{+}_{control}$	$CV_{lactate}$
4T1	12 ± 6 (1.2)∗	24	1.8 ± 1.5 (0.3)	27	85	$<10^{-5}$	0.48	0.80

∗ Mean ± SD (SEM)

+ Coefficient of variation

Table S6. pH of RPMI culture medium measured at different time points for different conditions

Sodium lactate	**pH 0h**	**Temp. (°C)**	**pH 24h**	**Temp. (°C)**	**pH 48h**	**Temp. (°C)**
0 mM	7.3	29.5	7.2	32.4	7.0	32
10 mM	7.2	33.1	7.2	32.9	7.1	31.6
15 mM	7.2	32.4	7.3	32.4	7.1	33.3
20 mM	7.2	33.3	7.3	32.1	7.1	32.9
25 mM	7.2	32.9	7.4	31.0	7.1	32.1
Hydrochloric acid	**pH 0h**	**Temp. (°C)**	**pH 24h**	**Temp. (°C)**	**pH 48h**	**Temp. (°C)**
0 mM	7.2	33.3	7.4	31.7	7.1	31.5
10 mM	6.9	32.5	7.0	32	7.0	31.7
15 mM	6.8	32	6.8	31.2	6.8	31.3
20 mM	6.6	31.3	6.6	31.0	6.7	30.9
25 mM	6.3	29.9	6.4	30.4	6.4	30.5
Lactic acid	**pH 0h**	**Temp. (°C)**	**pH 24h**	**Temp. (°C)**	**pH 48h**	**Temp. (°C)**
0 mM	7.3	30.9	7.5	29.9	7.4	33.6
10 mM	7.2	31.2	7.4	29	7.2	33.5
15 mM	7.1	29.8	7.2	28.5	7.1	33.7
20 mM	6.9	31.7	7.1	28.8	7.0	32.9
25 mM	6.8	31.7	6.9	29.6	6.9	33.3

Bibliography

[1] Pratx G et al. (2013) High-resolution radioluminescence microscopy of ^{18}F-FDG uptake by reconstructing the β-ionization track. Journal of Nuclear Medicine 54(10):1841– 1846.